Geochemistry
Geophysics
Geosystems
G3

Article
Volume 12, Number 10
20 October 2011
Q10012, doi:10.1029/2011GC003717
ISSN: 1525-2027

Published by AGU and the Geochemical Society

Subduction of young oceanic plates: A numerical study with application to aborted thermal-chemical plumes

Idael Francisco Blanco-Quintero
Departamento de Mineralogía y Petrología, Universidad de Granada, Fuentenueva s/n, E-18002 Granada, Spain (blanco@ugr.es)

Taras V. Gerya
Department of Geosciences, Swiss Federal Institute of Technology, CH-8093 Zurich, Switzerland

Department of Geology, Moscow State University, 119899 Moscow, Russia

Antonio García-Casco
Departamento de Mineralogía y Petrología, Universidad de Granada, Fuentenueva s/n, E-18002 Granada, Spain

Instituto Andaluz de Ciencias de la Tierra, CSIC, Universidad de Granada, Fuentenueva s/n, E-18002 Granada, Spain

Antonio Castro
Departamento de Geología, Universidad de Huelva, Campus del Carmen, E-21071 Huelva, Spain

[1] We investigated numerical models of initiation and subsequent evolution of subduction of young (10–30 Myr) oceanic lithosphere. Systematic numerical experiments were carried out by varying the age of the subducting plate (10, 12.5, 15, 17.5, 20, 25 and 30 Myr), the rate of induced convergence (2, 4 and 5 cm/yr) and the degree of hydration (0 and 2 wt% H_2O) of the pre-existing weak oceanic fracture zone along which subduction is initiated. Despite the prescribed plate forcing, spontaneously retreating oceanic subduction with a pronounced magmatic arc and a backarc basin was obtained in a majority of the experiments. It was also found that the younger age of oceanic lithosphere results in more intense dehydration and partial melting of the slab during and after the induced subduction initiation due to the shallow dispositions of the isotherms. Partial melting of the subducted young crust may create thermal-chemical instabilities (cold plumes) that ascend along the slab-mantle interface until they either freeze at depth or detach from the slab and penetrate the upper plate lithosphere contributing to the nucleation and growth of a volcanic arc. Freezing of the plumes in the slab-mantle interface is favored by subduction of very young lithosphere (i.e., 10 Myr) at moderate rate (4 cm/yr) of convergence. Such aborted plumes may correspond to Cretaceous partially melted MORB-derived slab material and associated adakitic tonalitic-trondhjemitic rocks crystallized at ca. 50 km depth in the slab-mantle interface and exhumed in a subduction channel (serpentinite mélanges) in eastern Cuba.

Components: 6700 words, 8 figures, 1 table.

Keywords: partial melting; serpentinite mélange; subduction initiation; thermal-chemical plumes; volcanic arc.

Index Terms: 0545 Computational Geophysics: Modeling (1952, 4255, 4316); 1031 Geochemistry: Subduction zone processes (3060, 3613, 8170, 8413); 1038 Geochemistry: Mantle processes (3621).

Received 24 May 2011; **Revised** 6 September 2011; **Accepted** 7 September 2011; **Published** 20 October 2011.

Blanco-Quintero, I. F., T. V. Gerya, A. García-Casco, and A. Castro (2011), Subduction of young oceanic plates: A numerical study with application to aborted thermal-chemical plumes, *Geochem. Geophys. Geosyst.*, *12*, Q10012, doi:10.1029/2011GC003717.

1. Introduction

[2] Subduction zones and mid ocean spreading ridges are the most important tectonic features in planet Earth, with more than 55,000 km and 60,000 km of integrated length respectively [*Lallemand*, 1999; *Stern*, 2002]. These biggest structures have significant influence in the transformation and evolution of the planet. Lithosphere formed at ridges is eventually recycled into the mantle by means of subduction. The geophysical characteristics of subduction zones are varied and controlled by factors like plate velocity, direction and angle of convergence, thickness and age of the lithosphere, convection in the overlying mantle wedge, fluids and melts migrating through the subduction zone, and time [e.g., *Kirby et al.*, 1991; *Peacock*, 1996]. These factors determine the evolution of subduction zone and subsequent formation of volcanic arcs, which ultimately contribute to the growing of continental masses.

[3] The addition of aqueous fluids to the mantle produces partial melting of peridotite at temperatures hundreds of degrees lower than under dry conditions [*Green*, 1973; *Kushiro et al.*, 1972; *Mysen and Boettcher*, 1975a, 1975b; *Ulmer*, 2001]. This addition takes place in convergent margins by means of dehydration of the subducting slab (crust and mantle) caused by increasing pressure and temperature. At the onset of subduction, the fluid released is primarily the result of the expulsion of connate water, but the oceanic crust may contain up to about 6 wt % water in chlorite, lawsonite and amphibole [*Iwamori*, 1998]. This amount is drastically reduced in the earliest 50 km during subduction by metamorphic dehydration reactions [e.g., *Iwamori*, 1998; *Schmidt and Poli*, 1998].

[4] When a young (i.e., hot) oceanic plate subducts, the geothermal gradient involved in the slab-mantle wedge interface is hotter compared to the geothermal gradient generated upon subduction of an old (i.e., cold) plate, making possible the intersection of the wet solidus of basaltic and pelitic rocks at moderate pressure (e.g., 15 kbar; 50 km). Partial melting of the slab at shallow depths has important consequences for the transformation of the mantle wedge and the evolution of volcanic arcs [e.g., *Peacock et al.*, 1994]. The addition of the slab melt to the wedge occurs either by melt percolation [e.g., *Scott and Stevenson*, 1986] and re-equilibration with the mantle or by means of thermal-chemical (cold) plumes resulting from Rayleigh-Taylor instabilities [*Gerya and Yuen*, 2003a], which may have genetic relations with adakite rocks formed at the surface as product of slab melting [*Defant and Drummond*, 1990; *Martin*, 1999] or granitoid magmas [*Castro and Gerya*, 2008; *Castro et al.*, 2010]. Under special circumstances, however, the slab melts may crystallize at depth and may be incorporated into subduction channels and be exhumed, allowing us the in situ characterization of slab-derived melts [e.g., *García-Casco et al.*, 2008; *Lázaro and García-Casco*, 2008].

[5] In this paper we study the onset of induced [e.g., *Stern*, 2004] intraoceanic subduction using different ages of lithosphere, initial convergence rates and degree of rock hydration in subduction initiation zone. To this end, we use a thermomechanical numerical model based on finite differences and marker-in-cell techniques [*Gerya and Yuen*, 2003b]. The model includes spontaneous slab retreat, subducted crust dehydration, aqueous fluid transport and slab and mantle wedge melting. The results, specially those concerning the formation and evolution of thermal-chemical plumes, are compared with rocks complexes occurring in the northern Caribbean (eastern Cuba), where partial melting of very young oceanic lithosphere shortly after onset of subduction has been recently described in serpentinite mélanges representing fragments of the Cretaceous Antillean subduction channel [*Blanco-Quintero et al.*, 2010; *García-Casco et al.*, 2008; *Lázaro and García-Casco*, 2008; *Lázaro et al.*, 2009].

2. Numerical Model Description and Governing Equations

[6] We developed a 2D thermomechanical numerical model of onset of intraoceanic subduction (Figure 1) using the I2VIS code based on conservative finite differences and non-diffusive marker-in-cell techniques [*Gerya and Yuen*, 2003b]. The experiments were conducted on Brutus computer cluster of ETH-Zurich. The model dimensions are 4000 km × 200 km, distributed over 2001 × 201 grid nodes. The grid resolution is non uniform with 1 km × 1 km resolution in the subduction region and 5 km × 1 km resolution at the model margins.

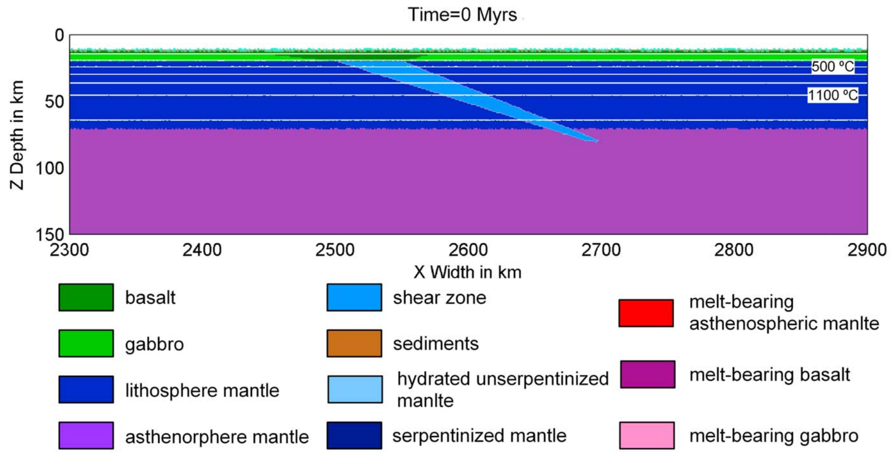

Figure 1. Initial configuration of the numerical model (see text for details). White lines are isotherms shown for increments of 200°C starting from 100°C. Colors indicate materials (e.g., rock type or melt) which appear in Figures 2–7. High-resolution central 600 × 150 km part of the original 4000 × 200 km model is shown.

[7] The oceanic crust consists of a 3 km thick layer of basalts and a 5 km thick layer of gabbroic rocks. The lithospheric and asthenospheric mantle is modeled as anhydrous peridotite, extending as a half-space to the lower boundary of the model. This setup is complemented by 2 km of water above and 10 km of air. Sedimentation spontaneously fills the trench after the arc-ward slope reaches 17° steepness.

[8] Subduction is initiated by a prescribed weak fracture zone between two oceanic plates (Figure 1). This zone is 50 to 10 km wide (taper) and reaching depth of 70 km. It consists of mantle rocks with wet olivine rheology [*Ranalli*, 1995] and low brittle/plastic strength (1 MPa). In the course of subduction, the mantle rocks of the fracture zone are replaced by weak crustal rocks and hydrated mantle, naturally preserving the localizing effect of the initially prescribed weak zone. Additionally, some experiments used intensely hydrated (up to 2 wt% H_2O) peridotite in the weak zone [e.g., *Gerya and Yuen*, 2003a; *Maresch and Gerya*, 2005; *Regenauer-Lieb et al.*, 2001] (Table 1).

[9] The initial temperature profile depends on the age of the lithosphere. In the evolution of the model water is expelled from the subducted oceanic crust as a consequence of dehydration reactions and compaction. Because the water transport model does not permit complete hydration of the peridotitic mantle, the mantle solidus is intermediate between the wet and dry peridotite solidus. In reality variable hydration would permit melting over a range of temperatures and water contents [e.g., *Grove et al.*, 2006].

[10] Three principal equations are used in the two dimensional creeping-flow models (momentum, continuity, and thermal equations). The conserva-

Table 1. Description of Numerical Experiments

Model	Slab Age (Myr)	Convergent Rate (cm/yr)	H_2O Content in the Weak Zone (wt %)
1	10	2	0
2	12.5	2	0
3	15	2	0
4	17.5	2	0
5	20	2	0
6	25	2	0
7	30	2	0
8	10	4	0
9	12.5	4	0
10	15	4	0
11	17.5	4	0
12	20	4	0
13	25	4	0
14	30	4	0
15	10	5	0
16	12.5	5	0
17	15	5	0
18	17.5	5	0
19	20	5	0
20	25	5	0
21	30	5	0
22	10	5	2
23	12.5	5	2
24	15	5	2
25	17.5	5	2
26	20	5	2
27	25	5	2
28	30	5	2

tion of mass is approximated by the incompressible continuity equation:

$$\frac{\partial v_x}{\partial x} + \frac{\partial v_z}{\partial z} = 0$$

The 2D Stokes equations take the form:

$$\frac{\partial \sigma_{xx}}{\partial x} + \frac{\partial \sigma_{xz}}{\partial z} = \frac{\partial P}{\partial x}$$

$$\frac{\partial \sigma_{zz}}{\partial z} + \frac{\partial \sigma_{xz}}{\partial x} = \frac{\partial P}{\partial z} - g\rho(T,P,C)$$

The density $\rho(T, P, C)$ depends explicitly on the temperature (T), the pressure (P) and the composition (C), and g is the gravitational acceleration.

[11] The Lagrangian temperature equation includes heat effects produced by phase transformations in the crust and mantle and is formulated as [*Gerya and Yuen*, 2003b]:

$$\rho C_P\left(\frac{DT}{Dt}\right) = -\frac{\partial q_x}{\partial x} - \frac{\partial q_z}{\partial z} + H_r + H_a + H_S + H_L,$$

$$q_x = -k(T,C)\frac{\partial T}{\partial x}$$

$$q_z = -k(T,C)\frac{\partial T}{\partial z}$$

$$H_a = T\alpha\frac{DP}{Dt}$$

$$H_S = \sigma_{xx}\dot{\varepsilon}_{xx} + \sigma_{zz}\dot{\varepsilon}_{zz} + 2\sigma_{xz}\dot{\varepsilon}_{xz}$$

where *D/Dt* is the substantive time derivative; x and z denote, respectively, the horizontal and vertical coordinates; σ_{xx}, σ_{xz}, σ_{zz} are components of the deviatoric stress tensor; $\dot{\varepsilon}_{xx}$, $\dot{\varepsilon}_{xz}$, $\dot{\varepsilon}_{zz}$ are components of the strain rate tensor; P is pressure; T is temperature; q_x and q_z are heat flux components; ρ is density; $k(T, C)$ is the thermal conductivity, a function of composition and temperature; Cp is the isobaric heat capacity; H_r, H_a, H_S and H_L denote, the radioactive, adiabatic, shear and latent heat production, respectively.

[12] In the experiments the melt migration is assumed to occur rapidly compared to the deformation of unmelted mantle, so that the velocity of the melt is independent of mantle dynamics [*Elliott et al.*, 1997; *Hawkesworth et al.*, 1997]. Therefore, the extracted melt is transported rapidly to the surface forming volcanic arc crust.

[13] The effective creep viscosities of rocks are represented as a function of temperature and stress by experimentally determined flow laws. The viscosity for dislocation creep depends on strain rate, pressure and temperature and is defined in terms of deformation invariants [*Ranalli*, 1995] as follows,

$$\eta_{creep} = (\dot{\varepsilon}_{II})^{(1-n)/n} F(A_D)^{-1/n} \exp\left(\frac{E+VP}{nRT}\right)$$

were $\varepsilon_{II} = \sqrt{1/2\dot{\varepsilon}_{ij}\dot{\varepsilon}_{ij}}$ is the second invariant of the strain rate tensor and A_D, E, V and n are the experimentally determined flow law parameters, the material constant, the activation energy, the activation volume and the stress exponent, respectively. F is a dimensionless coefficient depending on the type of experiments on which the flow law is based and is used for conversion of experimentally determined rheologies to model stress states. For example, $F = \frac{2^{(1-n)/n}}{3^{(1+n)2n}}$ for triaxial compression, and $F = 2^{(1-2n)/n}$ for simple shear.

[14] The ductile rheology is combined with a brittle rheology to yield an effective visco-plastic rheology. For this purpose the Mohr–Coulomb yield criterion [e.g., *Ranalli*, 1995] is implemented by limiting creep viscosity, η_{creep}, as follows:

$$\eta_{creep} \leq \frac{\sigma_{yield}}{2\varepsilon_{II}}$$

$$\sigma_{yield} = c + P\sin(\varphi)$$

$$\sin(\varphi) = \sin\left(\varphi_{dry}\right)\lambda_{fluid}$$

$$\lambda_{fluid} = 1 - \frac{P_{fluid}}{P_{solid}}$$

Therefore, the plastic strength depends on the mean stress on the solids, $P_{solid} = P$ (dynamic pressure), the cohesion, c, which is the strength at $P = 0$, and on the effective internal friction angle, φ, which is calculated from the friction angle of dry rocks, φ_{dry}, and the pore fluid pressure factor λ_{fluid}. This factor is interpreted as $\lambda_{fluid} = 1 - \frac{P_{fluid}}{P_{solid}}$; the pore fluid pressure P_{fluid} reduces the yield strength σ_{yield} of fluid-containing porous or fractured media. In our numerical experiments $\lambda_{fluid} = 0.001$, which implies strong decoupling in the forearc region [*Gerya and Meilick*, 2011]. Similarly, the weakening effect of ascending melts is included. During a melt extraction episode, the yield strength σ_{yield} of rock in the column between the source of the melt and the surface is decreased according to λ_{melt}, = 0.001, which corresponds to strong overriding plate weakening favoring the retreating subduction mode [*Gerya and Meilick*, 2011].

[15] Further details of petrological and rheological models, melt and fluid transport algorithms and

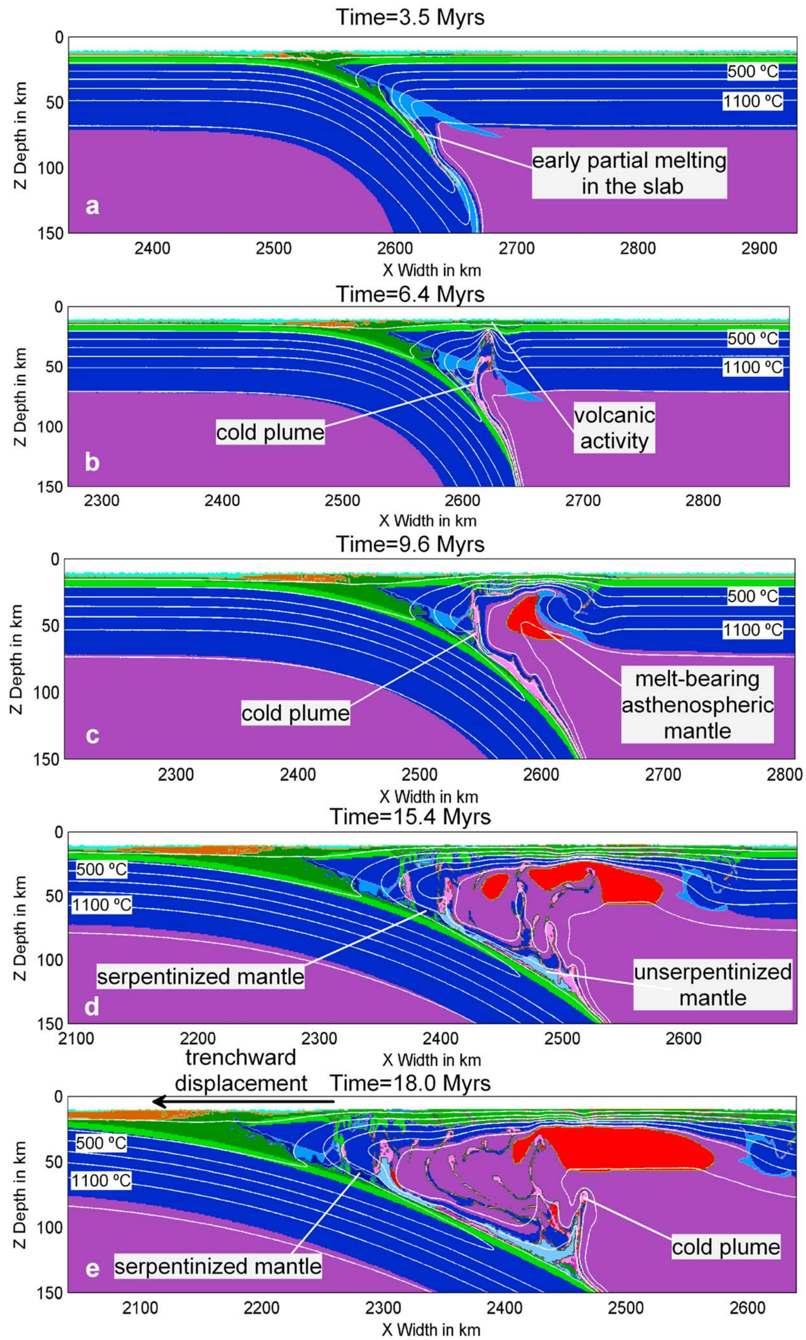

Figure 2. Evolution of the reference model. The model presents retreating subduction with the formation of (a) partial melts in the slab, (b) magmatic arc, (c) an extensional backarc basin with newly forming oceanic floor and slab retreat, and (d and e) evolution of the subduction zone. The age of the lithosphere is 10 Myr and initial convergence rate is 5 cm/yr.

boundary conditions are presented by *Sizova et al.* [2010] and *Gerya and Meilick* [2011].

3. Results

[16] Systematic numerical experiments were carried out by varying the age of the subducting plate (10, 12.5, 15, 17.5, 20, 25 and 30 Myr), the rate of convergence (2, 4 and 5 cm/yr) and the degree of hydration (0 and 2 wt% H_2O) of the weak zone (Table 1). The experiments were tested in order to analyze the influence of these parameters for the evolution of the subduction systems. Figure 2, constructed for the reference model with a lithosphere of 10 Myr and a convergence rate of 5 cm/yr, summarizes the basic features of the evolution in con-

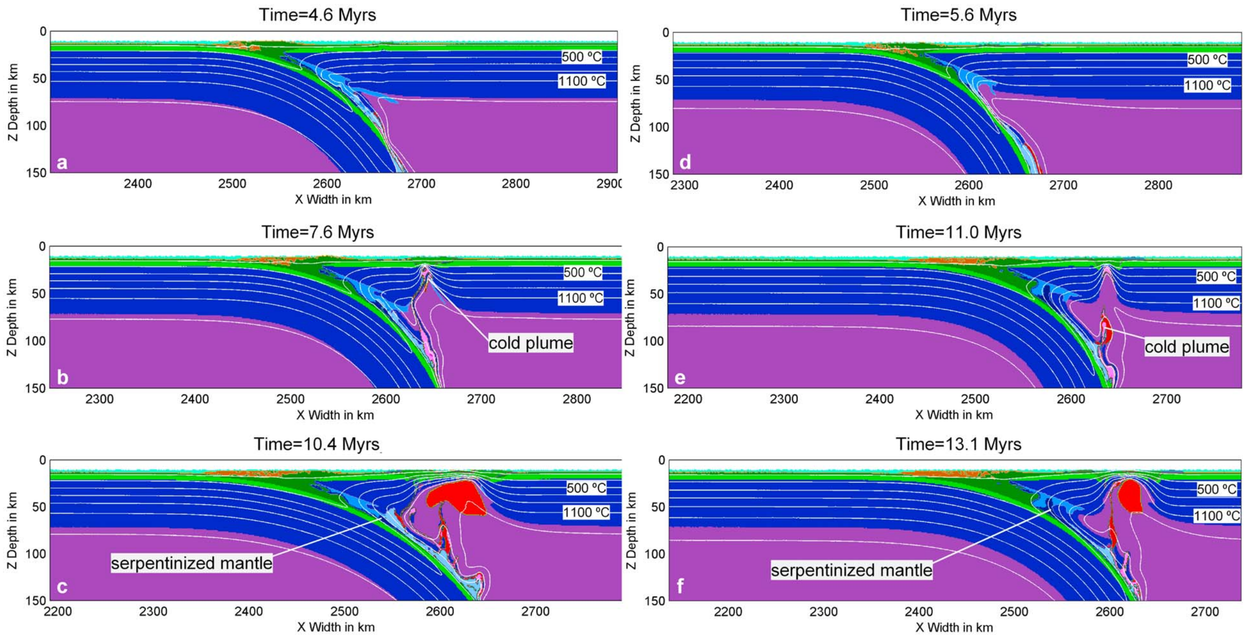

Figure 3. Snapshots from numerical experiments with different lithosphere age: (a–c) younger oceanic lithosphere (12.5 Myr) and (d–f) oceanic lithosphere of 15 Myr.

ducted experiments, including the trenchward displacement and deformation of the overriding plate, the increase in the slab angle, the hydration (serpentinization) of the mantle wedge and development of a subduction channel, the generation of molten rocks in the mantle wedge, the development of molten compositionally buoyant thermal-chemical (cold) plumes and waves along the subduction zone, and the displacement of isotherms (cooling of the subduction zone, heating of the volcanic arc region) with time. The model produces a spontaneously retreating trench with formation of a magmatic arc and extensional backarc basin with newly forming oceanic floor. When the subducting oceanic plate reaches approximately 50 km depth, dehydration and fluid flow leads to hydration and wet melting of the mantle above the slab, in agreement with common views of evolution of subduction zones [*Stern*, 2002, 2004; *van Keken et al.*, 2002]. However, this process first produces upwelling partially molten thermal-chemical plumes [*Gerya and Yuen*, 2003a] that rise from the slab along the slab-mantle interface until they penetrate the upper plate lithospheric mantle (Figures 2b–2e) weakened by migration of melts extracted toward the surface [*Sizova et al.*, 2010; *Gerya and Meilick*, 2011]. These plumes are composed of mixed hydrated partially molten components from the subducted crust and the mantle wedge [*Castro et al.*, 2010; *Gerya and Yuen*, 2003a; *Gorczyk et al.*, 2007].

[17] Rising of cold plumes lead to the growth of a magmatic arc at the surface of the overriding oceanic plate ~6 Myr after beginning of subduction (Figure 2b). As the trench retreats the melt-bearing asthenosphere rises forming an intra-arc spreading center leading to splitting of the arc and development of a remnant arc located trenchward and a back-arc basin (~10 Myr; Figure 2c). The formation of a spreading center accelerates trench retreat since it breaks apart the initially coherent overriding plate. The appearance of a melt-bearing mantle region below the spreading center (cf. broad red region in Figures 2c–2e) is driven by decompression melting.

[18] The age of the subducting lithosphere has a strong influence for the evolution of the subduction zone (Figure 3). For the same convergence rate, subduction of older lithosphere delays slab retreat, partial melting of the slab and rise of cold plumes. This change in the timing of the events on the order of a few million years is observed even for small variations in the age of the lithosphere (Figure 3; lithosphere ages of 12.5 Myr and 15 Myr; convergence rate 5 cm/yr). The volcanic activity is consequently affected, mostly because the time needed for dehydration of the slab and development of cold plumes is shortened for younger subducting lithosphere. Also the thermal-chemical plumes are rooted at greater depth in older lithosphere (Figure 3f).

[19] The rate of convergence between plates also influences the evolution of the subduction zone. For

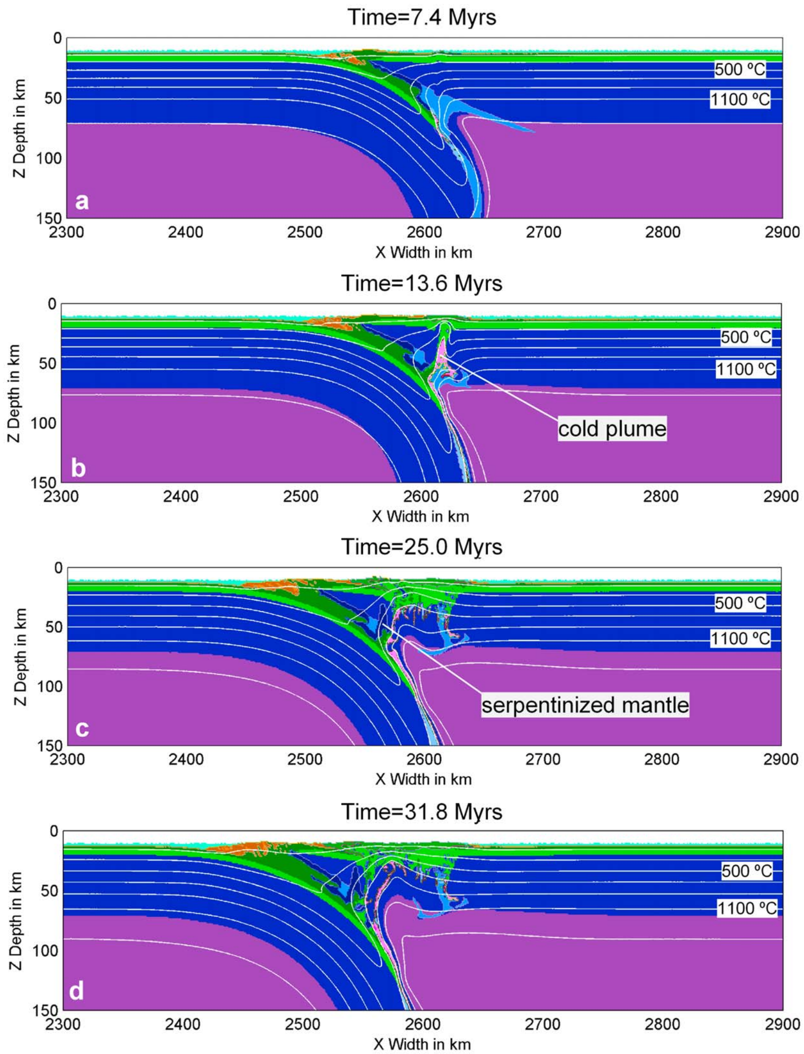

Figure 4. Numerical experiments with small initial convergence rate (2 cm/yr) and a lithosphere of 10 Myr. In these experiments, partial melting of the slab, formation of cold plumes and volcanic activity are delayed relative to faster convergence rates. No slab retreat and back arc formation is observed.

smaller convergence rates (e.g., ca. 2 cm/yr) slab retreat is not produced (Figure 4) for very young oceanic lithosphere (<20 Myr). However, the most important effect is related to partial melting of the slab and the beginning of volcanic arc activity, which are delayed (Figures 4a and 4b). Because the slab does not retreat in these models, the arc experiences focused magmatism and negligible amount of extension during more than 30 Myr after the onset of subduction (Figure 4d), producing large piles of volcanic rocks. In contrast, for older lithosphere (>20 Ma) and small convergence rate (2 cm/yr) the model predicts subtle slab retreat, regional dispersion of volcanic arc products, and formation of a backarc spreading center (Figure 5). It is important to note the depression of the isotherms, yielding slab melting and cold plume formation at greater depth.

[20] To evaluate the influence of an intense hydration (serpentinization) of pre-existing weak zone at shallow depths (<30 km), experiments were carried out for a weak zone composed of hydrated peridotite initially containing 2 wt% of water at sub-solidus conditions. In these experiments, partial melting of the weak rock above (i.e., deeper) the antigorite stability field (wet peridotite) takes place shortly after onset of subduction (Figure 6a). However, melt volume is small and is dissipated in the mantle (Figure 6b). After this early stage, the evolution of the subduction system follows a normal regime as described above. However, the volcanic arc activity occurs later than in other experiments (Figure 6c) and, importantly, a large serpentinized mantle (subduction channel) is formed above the slab (Figures 6d and 6e) due to large fluid flux from the hydrated

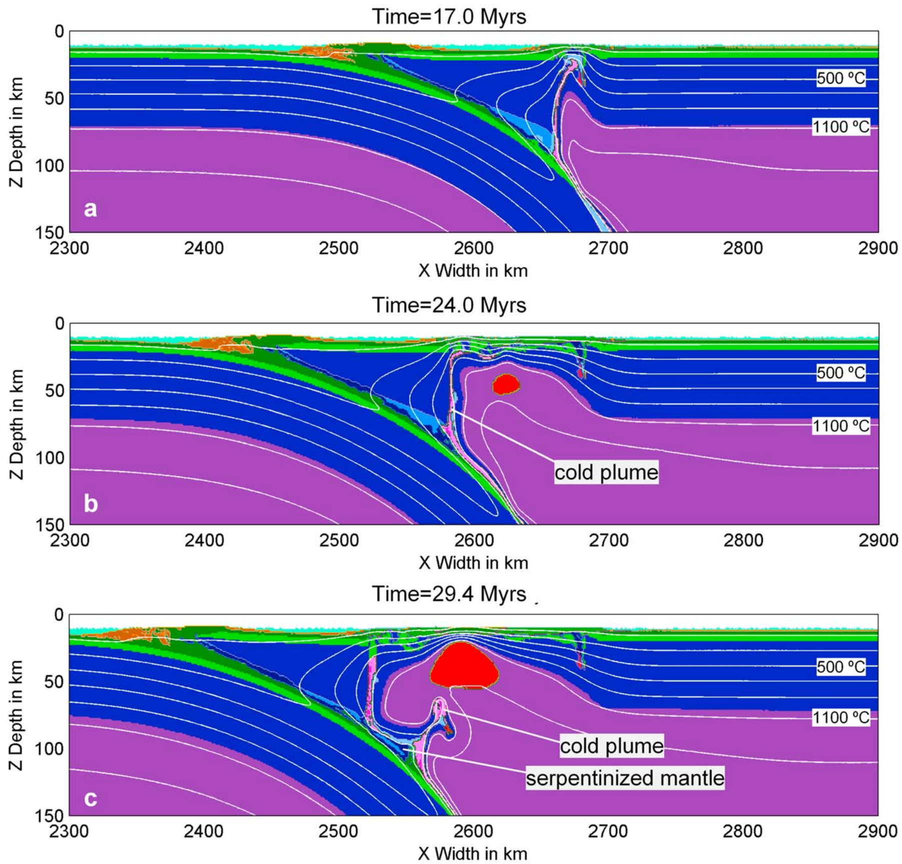

Figure 5. Numerical experiments with small convergence rate (2 cm/yr) and a lithosphere of 25 Myr. Slab retreat and backarc spreading occur relatively late.

peridotite initially present inside the subduction initiation zone.

[21] Finally, models for very young lithosphere yield small melt fractions in the partially molten slab at moderate depth and relatively low temperature. This setting allows crystallization of the cold plume at depth. This is illustrated in Figure 7 for a lithosphere of 10 Myr and an initial convergence rate of 4 cm/yr. In this experiment, the low proportions of melt produced preclude the rise of the plume through mantle, and the cooling of the system upon continued subduction leads to crystallization of the melt at depth close to the region where the plume nucleated at the slab-mantle wedge interface (50–60 km; Figure 7). We name this type of thermal-chemical plumes crystallized at depth as aborted plumes.

4. Discussion

4.1. Cold Plumes and Aborted Cold Plumes

[22] Subduction of very young oceanic lithosphere and ridges is a normal process of active margins [e.g., *Thorkelson and Breitsprecher*, 2005]. The thermal structure and melting of young subducted slabs was modeled by *Peacock et al.* [1994], and *Peacock* [1996] provided a general conceptual model for melting of young oceanic crust. However, in these experiments thermal steady state subduction models were explored and melting occurred only for very young crust (<5 Myr) [*Peacock et al.*, 1994]. Subduction of very young oceanic lithosphere has been also linked to the generation of adakites, based on geochemical data [e.g., *Defant and Drummond*, 1990; *Martin*, 1999] and numerical models [e.g., *Peacock et al.*, 1994; *Sizova et al.*, 2010]. The data compiled by *Drummond and Defant* [1990], summarizing adakite occurrences, suggest that melting occurs in slabs as old as 20 Myr. Such possibility is also identified by thermomechanical experiments with kinematically prescribed slabs [*Kelemen et al.*, 2004].

[23] Our experiments indicate that in nonsteady state, self consistent thermomechanical models partial melting occurs in slabs as old as 20–30 Myr shortly after the induced subduction initiation.

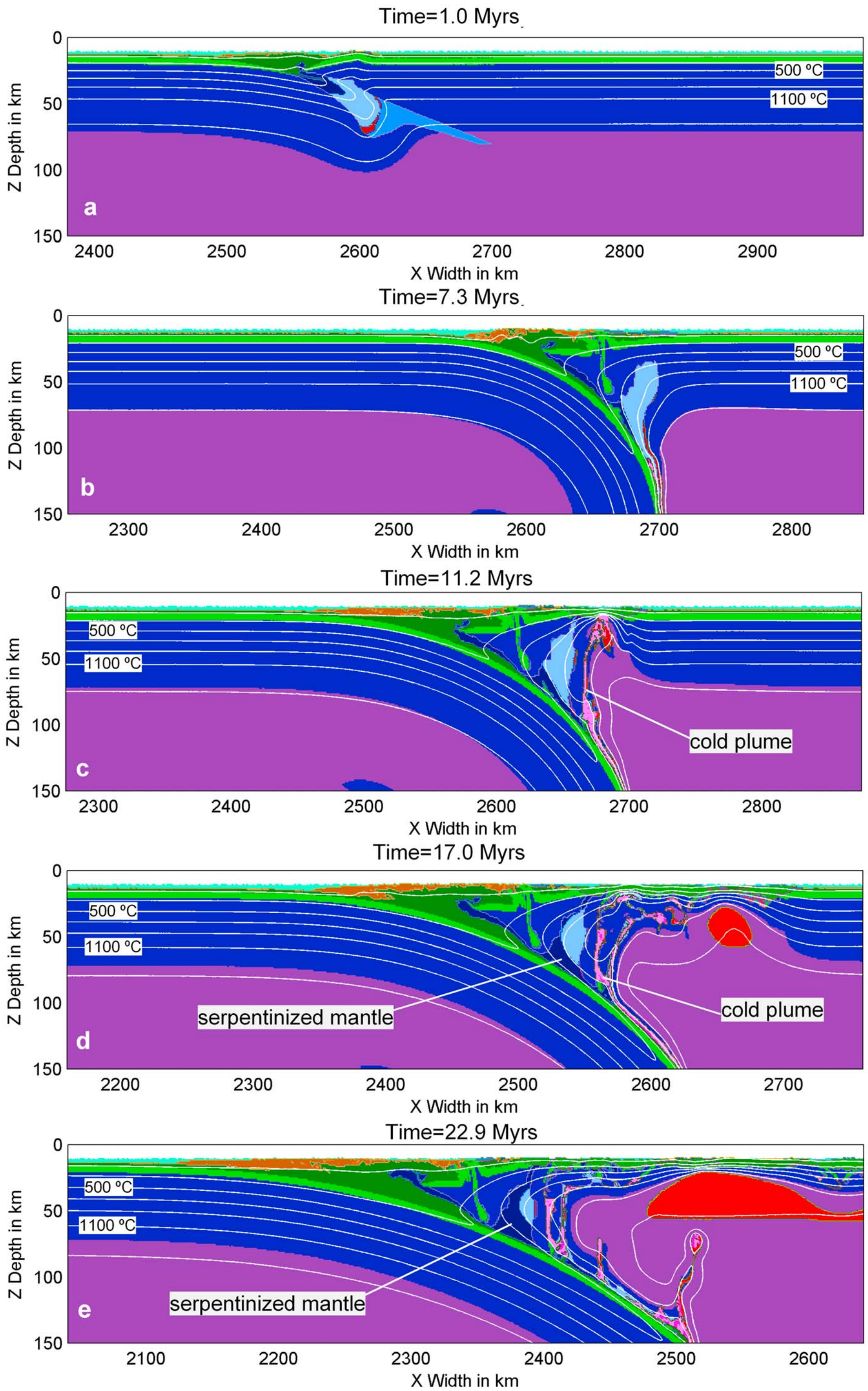

Figure 6. Numerical experiments with the weak zone composed of hydrated peridotite, age of lithosphere of 10 Myr, and initial convergence rate of 5 cm/yr.

However, it occurs earlier and at shallower depths in younger slabs (due to the shallow dispositions of the isotherms) and determining the evolution of volcanic arcs and back-arc basins. Hydrated, partially molten thermal-chemical plumes are responsible for the heterogeneous composition of the mantle wedge and influence the composition of the volcanic arc crust [*Castro et al.*, 2010; *Gerya and Yuen*, 2003a; *Gorczyk et al.*, 2007].

[24] However, we have also shown that under special circumstances cold plumes may crystallize

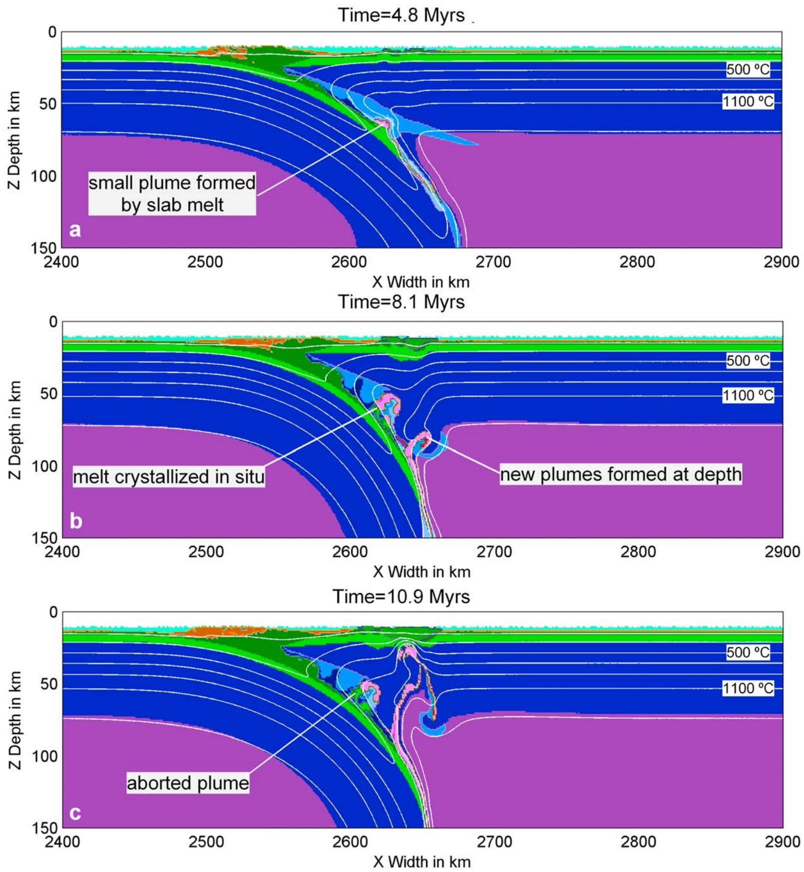

Figure 7. Example of aborted thermal-chemical plume development. The experiment represents a lithosphere of 10 Myr with an initial convergence rate of 4 cm/yr.

at depth in the slab-wedge region shortly after onset of subduction. These plumes have no significant influence on the evolution of the upper plate mantle and arc crust, but this type of aborted plumes may offer important information on the partial melting processes and the composition of melts that are potential metasomatic agents to modify the suprasubduction mantle wedge. Exhumation of this type of plumes is favored as they freeze at relatively shallow depth (ca. 50 km) in a region close to the slab-wedge interface, where a serpentinitic subduction channel is generated with time providing the mechanism for syn-subduction exhumation of accreted material [*Gerya et al.*, 2002].

[25] An example of partially molten subducted oceanic material incorporated in a subduction channel is found in the Catalina Schists of the Franciscan belt [*Bebout and Barton*, 2002; *Sorensen*, 1988; *Sorensen and Barton*, 1987; *Sorensen and Grossman*, 1989]. However, a more spectacular example, with larger proportion of melt, has been recently described in the serpentinitic mélanges of eastern Cuba (Sierra del Convento and La Corea mélanges) [*Blanco-Quintero et al.*, 2010, 2011a; *García-Casco et al.*, 2008; *Lázaro and García-Casco*, 2008; *Lázaro et al.*, 2009]. The model show here offers a plausible thermomechanical explanation for these important complexes in which it is possible to observe aborted processes of melt migration during subduction.

4.2. Comparing a Theoretical and a Natural Aborted Cold Plume (Eastern Cuba)

[26] A belt of Cretaceous-Tertiary volcanic arc rocks occurring all along the entire Caribbean region, from Guatemala, Greater, Lesser, Leeward and Netherland Antilles, northern Venezuela and north and western Colombia (collectively termed "Great Arc of the Caribbean" [*Burke*, 1988]) document a long lasting history of oceanic subduction in this region (Figure 8a). Ophiolitic materials of back-arc, arc, fore-arc and abyssal origin are also represented along the belt (for review see *Lewis et al.* [2006]). Associated with these rocks appear serpentinite matrix mélanges with high-pressure tectonic blocks that represent the associated Caribbean subduction channel. Cold, warm and hot subduction

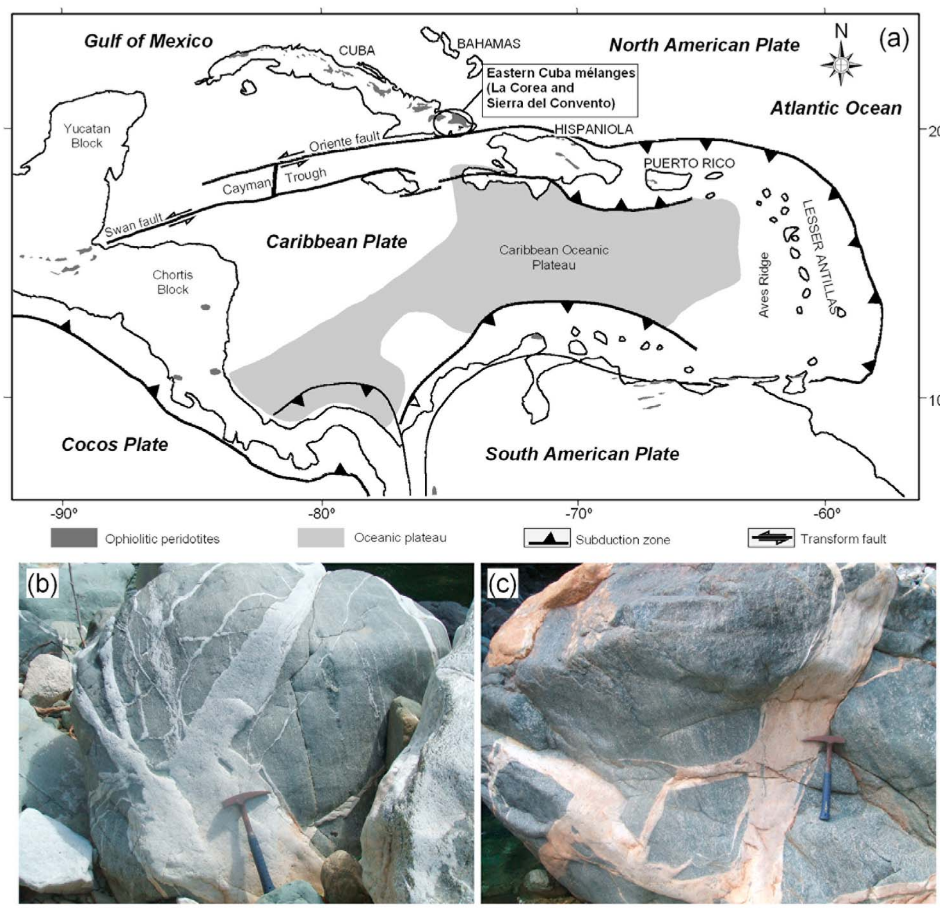

Figure 8. (a) Plate tectonic configuration of the Caribbean region, including ophiolitic bodies; the location of eastern Cuba mélanges are indicated. (b and c) Tonalite-trondhjemite veins crosscutting amphibolitic blocks.

has been inferred from petrological studies of these mélanges [e.g., *Brueckner et al.*, 2009; *García-Casco et al.*, 2002, 2006, 2008; *Krebs et al.*, 2008; *Maresch et al.*, 2009; *Tsujimori et al.*, 2005, 2006].

[27] In eastern Cuba, the La Corea and Sierra del Convento mélanges [*García-Casco et al.*, 2006; *Somin and Millán*, 1981] bear evidence for hot subduction, interpreted as the result of onset of subduction of young oceanic lithosphere [*Blanco-Quintero et al.*, 2010; *García-Casco et al.*, 2008; *Lázaro et al.*, 2009]. These mélanges are characterized by the presence of subducted MORB-derived epidote ± garnet amphibolite blocks associated with tonalitic-trondhjemitic-granitic bodies and veins (Figures 8b and 8c) generated after partial melting of the amphibolites and crystallized at depth (ca. 50 km; 15 kbar; 700–750°C). The rocks followed counter-clockwise P-T paths documenting subduction shortly after onset of subduction and slow syn-subduction exhumation in a subduction channel. Following our results of numerical experiments (i.e., Figure 7), we consider these blocks of high-grade amphibolite and associated leucocratic igneous rocks as possible fragments of an aborted cold plume incorporated into the Caribbean subduction channel.

[28] These high pressure igneous rocks (tonalites-trondhjemites) have some geochemical characteristics comparable to Cenozoic adakites [*Defant and Drummond*, 1990; *Martin*, 1999], including depletion in HREE and enrichment in LREE and positive Eu anomaly in the REE patterns, high Sr/Y, SiO_2 > 56 wt %, Al_2O_3 > 15 wt %, $Sr^{87}/Sr^{86} < 0.7040$, but very low Yb < 1 ppm, Y < 10 ppm and $(La/Yb)_n < 17$ [see *Blanco-Quintero et al.*, 2011b; *Lázaro and García-Casco*, 2008; *Lázaro et al.*, 2011]. The Sr and Nd isotopic composition clearly indicate that these rocks were produced by fluid-fluxed partial melting of MORB-amphibolite blocks (i.e., host rocks) with no input of external sources [*Lázaro and García-Casco*, 2008]. These chemical features are explained by residual garnet and amphibole and complete consumption of plagioclase in the source

(i.e., the melt residue), characteristic of the MORB-amphibolites of eastern Cuba mélanges. The peraluminous character of the leucocratic rocks [*Blanco-Quintero et al.*, 2011b; *García-Casco et al.*, 2008; *Lázaro and García-Casco*, 2008] also supports an origin at moderate temperature conditions close to the wet basaltic solidus, as indicated by experimental work [e.g., *Nakajima and Arima*, 1998; *Prouteau et al.*, 2001]. However, mild differences with adakites (e.g., very low Yb, Y, La and $(La/Yb)_n$) make these rocks more similar to the acid rocks from Catalina Schist mélange (California) considered to be primary slab melts [e.g., *Sorensen and Grossman*, 1989]. Consequently, the tonalitic-trondhjemitic rocks represent pristine slab melt [*Lázaro and García-Casco*, 2008], in agreement with results of the numerical models and make tonalitic-tronchjemitic rocks from eastern Cuba mélanges the most extended areas where in situ pristine slab melt have been described.

[29] Subduction rates for the Caribbean region during the Cretaceous have been estimated on the order of 2–4 cm/yr [*Krebs et al.*, 2008, and references therein]. These figures are in agreement with our models, since they allow slab retreat and backarc basin formation, and petrological and geochemical data have shown that Mayarí-Baracoa Ophiolitic Belt of eastern Cuba formed at a back-arc spreading center [*Marchesi et al.*, 2006]. Furthermore, subduction of hot young oceanic lithosphere during the Cretaceous is incorporated in geodynamic models for the region [*Pindell and Kennan*, 2009]. In these geodynamic models, subduction involved the Proto-Caribbean basin (Atlantic), which was opening at that time due to North America and South America drift, and subduction of a young lithosphere or ridge was possible. Accordingly, we consider the model presented in Figure 7 involving subduction of very young oceanic lithosphere (10 Myr) at a rate of 4 cm/yr as potentially feasible for eastern Cuba in the early Cretaceous (ca. 120 Ma) [*Blanco-Quintero et al.*, 2011b; *Lázaro et al.*, 2009], and the predicted formation of an aborted cold plume as an analog of the partially melted slab rocks found in eastern Cuba mélanges.

5. Conclusions

[30] Thermomechanical experiments were used to model intraoceanic subduction initiation induced by forcing of plate convergence across a pre-existing weak oceanic fracture zone. Experiments were carried out by varying the age of the lithosphere from 10 to 30 Myr and convergence rate from 2 to 5 cm/yr, influencing slab retreat and back-arc basin formation and evolution. For younger oceanic lithosphere, more intense dehydration and partial melting of the slab are produced. The volcanic arc crust initially forms as a response of intrusion of cold plumes into the upper plate lithosphere, with later evolutions influenced by decompression melting of rising asthenosphere. Partial melting of subducted material and volcanic arc activity is delayed for very low convergence rates. Experiments for subduction of very young lithosphere (i.e., 10 Myr) at moderate rate (4 cm/yr) of induced convergence allow formation of aborted thermal-chemical plumes in the slab-mantle interface, which have no significant influence on the evolution of the mantle wedge and arc crust. The predicted aborted plumes may correspond to Cretaceous partially melted MORB-derived slab material and associated adakitic tonalitic-trondhjemitic rocks crystallized at ca. 50 km depth in the slab-mantle interface and exhumed in a subduction channel (serpentinite mélanges) in eastern Cuba.

Acknowledgments

[31] We appreciated constructive comments by Erin Burkett and an anonymous reviewer and recommendations of Editor T. Becker. Blanco-Quintero would like to thank E. Sizova and Y. Mishin for provision of visualization routines, basic instructions and help during his stay in the ETH. We appreciate financial support from Spanish MCINN project CGL2009–12446 and support from Swiss National Science Foundation research grants 200020_129487, 200020_126832, 200021_113672/1, 200021_116381/1, 4D-Adamello, Swiss Federal Institute of Technology research grants ETH-06 09–2, ETH-08 07–2 and Crystal2Plate program to TVG. This is a contribution to IGCP-546 "Subduction zones of the Caribbean." Blanco-Quintero is supported by grant AP2005–5258 from the "Programa de Formación del Profesorado Universitario" of the Spanish Ministry of Education.

References

Bebout, G. E., and M. D. Barton (2002), Tectonic and metasomatic mixing in a high-T, subduction-zone mélange insights into the geochemical evolution of the slab-mantle interface, *Chem. Geol.*, *187*, 79–106, doi:10.1016/S0009-2541(02)00019-0.

Blanco-Quintero, I. F., A. García-Casco, Y. Rojas-Agramonte, A. Rodríguez-Vega, C. Lázaro, and M. A. Iturralde-Vinent (2010), Metamorphic evolution of subducted hot oceanic crust, La Corea mélange, Cuba, *Am. J. Sci.*, *310*, 889–915, doi:10.2475/11.2010.01.

Blanco-Quintero, I. F., C. Lázaro, A. García-Casco, J. Proenza, and Y. Rojas-Agramonte (2011a), Barium-rich fluids and melts in the subduction environment (La Corea and Sierra del Convento mélanges, eastern Cuba), *Contrib. Mineral. Petrol.*, *162*, 395–413, doi:10.1007/s00410-010-0603-2.

Blanco-Quintero, I. F., Y. Rojas-Agramonte, A. García-Casco, A. Kröner, D. F. Mertz, C. Lázaro, J. Blanco-Moreno, and P. R. Renne (2011b), Timing of subduction and exhumation in a subduction channel: Evidence from slab melts from La Corea mélange (eastern Cuba), *Lithos*, doi:10.1016/j.lithos.2011.08.009, in press.

Brueckner, H. K., H. G. Avé Lallemant, V. B. Sisson, G. E. Harlow, S. R. Hemming, U. Martens, T. Tsujimori, and S. S. Sorensen (2009), Metamorphic reworking of a high pressure–low temperature mélange along the Motagua fault, Guatemala: A record of Neocomian and Maastrichtian transpressional tectonics, *Earth Planet. Sci. Lett.*, *284*, 228–235, doi:10.1016/j.epsl.2009.04.032.

Burke, K. (1988), Tectonic evolution of the Caribbean, *Annu. Rev. Earth Planet. Sci.*, *16*, 201–230, doi:10.1146/annurev.ea.16.050188.001221.

Castro, A., and T. V. Gerya (2008), Magmatic implications of mantle wedge plumes: Experimental study, *Lithos*, *103*, 138–148, doi:10.1016/j.lithos.2007.09.012.

Castro, A., T. V. Gerya, A. García-Casco, C. Fernández, J. Diaz-Alvarado, I. Moreno-Ventas, and I. Löw (2010), Melting relations of MORB-sediment mélanges in underplated mantle wedge plumes. Implications for the origin of cordilleran-type batholiths, *J. Petrol.*, *51*, 1267–1295, doi:10.1093/petrology/egq019.

Defant, M. J., and M. S. Drummond (1990), Derivation of some modern arc magmas by melting of young subducted lithosphere, *Nature*, *347*(6294), 662–665, doi:10.1038/347662a0.

Drummond, M. S., and M. J. Defant (1990), A model for trondhjemite-tonalite-dacite genesis and crustal growth via slab melting: Archean to modern comparisons, *J. Geophys. Res.*, *95*, 21,503–21,521, doi:10.1029/JB095iB13p21503.

Elliott, T., T. Plank, A. Zindler, W. Wjite, and B. Bourdon (1997), Element transport from slab to volcanic front at the Mariana arc, *J. Geophys. Res.*, *102*, 14,991–15,019, doi:10.1029/97JB00788.

García-Casco, A., R. L. Torres-Roldán, G. Millán, P. Monié, and J. Schneider (2002), Oscillatory zoning in eclogitic garnet and amphibole, Northern Serpentinite Melange, Cuba: A record of tectonic instability during subduction?, *J. Metamorph. Geol.*, *20*, 581–598, doi:10.1046/j.1525-1314.2002.00390.x.

García-Casco, A., R. L. Torres-Roldán, M. A. Iturralde-Vinent, G. Millán, K. Núñez Cambra, C. Lázaro, and A. Rodríguez Vega (2006), High pressure metamorphism of ophiolites in Cuba, *Geol. Acta*, *4*, 63–88.

García-Casco, A., C. Lázaro, Y. Rojas-Agramonte, A. Kröner, R. L. Torres-Roldán, K. Núñez, G. Millán, F. Neubauer, and I. F. Blanco-Quintero (2008), Partial melting and counterclockwise P-T path of subducted oceanic crust (Sierra del Convento mélange, Cuba), *J. Petrol.*, *49*, 129–161, doi:10.1093/petrology/egm074.

Gerya, T. V., and F. I. Meilick (2011), Geodynamic regimes of subduction under an active margin: Effects of rheological weakening by fluids and melts, *J. Metamorph. Geol.*, *29*, 7–31, doi:10.1111/j.1525-1314.2010.00904.x.

Gerya, T. V., and D. A. Yuen (2003a), Rayleigh-Taylor instabilities from hydration and melting propel cold plumes at subduction zones, *Earth Planet. Sci. Lett.*, *212*, 47–62, doi:10.1016/S0012-821X(03)00265-6.

Gerya, T. V., and D. A. Yuen (2003b), Characteristics-based marker-in-cell method with conservative finite-differences schemes for modelling geological flows with strongly variable transport properties, *Phys. Earth Planet. Inter.*, *140*, 293–318, doi:10.1016/j.pepi.2003.09.006.

Gerya, T. V., B. Stoeckhert, and A. L. Perchuk (2002), Exhumation of high-pressure metamorphic rocks in a subduction channel: A numerical simulation, *Tectonics*, *21*(19), 1056, doi:10.1029/2002TC001406.

Gorczyk, W., T. V. Gerya, J. A. D. Connolly, and D. A. Yuen (2007), Growth and mixing dynamics of mantle wedge plumes, *Geology*, *35*, 587–590, doi:10.1130/G23485A.1.

Green, D. H. (1973), Experimental melting studies on a model upper mantle composition at high pressure under water-saturated and water-undersaturated conditions, *Earth Planet. Sci. Lett.*, *19*, 37–53, doi:10.1016/0012-821X(73)90176-3.

Grove, T. L., N. Chatterjee, S. W. Parman, and E. Medard (2006), The influence of H2O on mantle wedge melting, *Earth Planet. Sci. Lett.*, *249*, 74–89, doi:10.1016/j.epsl.2006.06.043.

Hawkesworth, C. J., S. P. Turner, F. McDermott, D. W. Peate, and P. van Calsteren (1997), U–Th isotopes in arc magmas: Implications for element transfer from the subducted crust, *Science*, *276*, 551–555, doi:10.1126/science.276.5312.551.

Iwamori, H. (1998), Transportation of H_2O and melting in subduction zones, *Earth Planet. Sci. Lett.*, *160*(1–2), 65–80, doi:10.1016/S0012-821X(98)00080-6.

Kelemen, P. B., J. L. Rilling, E. M. Parmentier, L. Mehl, and B. R. Hacker (2004), Thermal structure due to solid-state flow in the mantle wedge beneath arcs, in *Inside the Subduction Factory*, *Geophys. Monogr. Ser.*, vol. 138, edited by J. M. Eiler, pp. 293–311, AGU, Washington, D. C.

Kirby, S. H., W. B. Durham, and L. A. Stern (1991), Mantle phase changes and deep-earthquake faulting in subducting lithosphere, *Science*, *252*, 216–225, doi:10.1126/science.252.5003.216.

Krebs, M., W. V. Maresch, H. P. Schertl, A. Baumann, G. Draper, B. Idleman, and C. Münker (2008), The dynamics of intra-oceanic subduction zones: A direct comparison between fossil petrological evidence (Rio San Juan Complex, Dominican Republic) and numerical simulation, *Lithos*, *103*, 106–137, doi:10.1016/j.lithos.2007.09.003.

Kushiro, I., N. Shimizu, and Y. Nakamura (1972), Compositions of coexisting liquid and solid phases formed upon melting of natural garnet and spinel lherzolites at high pressures: A preliminary report, *Earth Planet. Sci. Lett.*, *14*, 19–25, doi:10.1016/0012-821X(72)90073-8.

Lallemand, S. (1999), *La Subduction Oceanique*, Gordon and Breach, Newark, N. J.

Lázaro, C., and A. García-Casco (2008), Geochemical and Sr-Nd isotope signatures of pristine slab melts and their residues (Sierra del Convento mélange, eastern Cuba), *Chem. Geol.*, *255*, 120–133, doi:10.1016/j.chemgeo.2008.06.017.

Lázaro, C., A. García-Casco, F. Neubaurer, Y. Rojas-Agramonte, A. Kröner, and M. A. Iturralde-Vinent (2009), Fifty-five-million-year history of oceanic subduction and exhumation at the northern edge of the Caribbean plate (Sierra del Convento mélange, Cuba), *J. Metamorph. Geol.*, *27*, 19–40, doi:10.1111/j.1525-1314.2008.00800.x.

Lázaro, C., I. F. Blanco-Quintero, C. Marchesi, D. Bosch, Y. Rojas-Agramonte, and A. García-Casco (2011), The imprint of subduction fluids on subducted MORB-derived melts (Sierra del Convento Mélange, Cuba), *Lithos*, *126*, 341–354, doi:10.1016/j.lithos.2011.07.011.

Lewis, J. F., G. Draper, J. A. Proenza, J. Espaillat, and J. Jimenez (2006), Ophiolite-related ultramafic rocks (serpentinites) in the Caribbean region: A review of their occurrence, composition, origin, emplacement and Ni-laterite soils formation, *Geol. Acta*, *4*, 237–263.

Marchesi, C., C. J. Garrido, M. Godard, J. A. Proenza, F. Gervilla, and J. Blanco-Moreno (2006), Petrogenesis of highly depleted peridotites and gabbroic rocks from the Mayarí-Baracoa Ophiolitic Belt (eastern Cuba), *Contrib. Mineral. Petrol.*, *151*, 717–736, doi:10.1007/s00410-006-0089-0.

Maresch, W. V., and T. V. Gerya (2005), Blueschists and blue amphiboles: How much subduction do they need?, *Int. Geol. Rev.*, *47*, 688–702, doi:10.2747/0020-6814.47.7.688.

Maresch, W. V., R. Kluge, A. Baumann, J. L. Pindell, G. Krückhans-Lueder, and K. Stanek (2009), The occurrence and timing of high-pressure metamorphism on Margarita Island, Venezuela: A constraint on Caribbean-South America interaction, in *The Origin and Evolution of the Caribbean Plate*, edited by K. H. James, M. A. Lorente, and J. L. Pindell, *Geol. Soc. Spec. Publ.*, *328*, 705–741.

Martin, H. (1999), The adakitic magmas: Modern analogues of Archaean granitoids, *Lithos*, *46*(3), 411–429, doi:10.1016/S0024-4937(98)00076-0.

Mysen, B. O., and A. L. Boettcher (1975a), Melting of a hydrous mantle. I. Phase relations of natural peridotite at high P and T and with controlled addition of water, carbon dioxide and hydrogen, *J. Petrol.*, *16*, 520–548.

Mysen, B. O., and A. L. Boettcher (1975b), Melting of a hydrous mantle. II. Geochemistry of crystals and liquids formed by anatexis of mantle peridotite at high pressure and high temperature as a function of controlled activities of water, hydrogen and carbon dioxide, *J. Petrol.*, *16*, 549–593.

Nakajima, K., and M. Arima (1998), Melting experiments on hydrous low-K tholeiite: Implications for the genesis of tonalitic crust in the Izu-Bonin-Mariana arc, *Isl. Arc*, *7*, 359–373, doi:10.1111/j.1440-1738.1998.00195.x.

Peacock, S. M. (1996), Thermal and petrologic structure of subduction zones, in *Subduction: Top to Bottom*, *Geophys. Monogr. Ser.*, vol. 96, edited by G. E. Bebout, D. School, and S. Kirby, pp. 119–133, AGU, Washington, D. C.

Peacock, S. M., T. Rushmer, and A. B. Thompson (1994), Partial melting of subducting oceanic crust, *Earth Planet. Sci. Lett.*, *121*, 227–244, doi:10.1016/0012-821X(94)90042-6.

Pindell, J., and L. Kennan (2009), Tectonic evolution of the Gulf of Mexico, Caribbean and northern South America in the mantle reference frame: An update, in *The Origin and Evolution of the Caribbean Plate*, edited by K. H. James, M. A. Lorente, and J. L. Pindell, *Geol. Soc. Spec. Publ.*, 328, 1–55.

Prouteau, G., B. Scaillet, M. Pichavant, and R. C. Maury (2001), Evidence for mantle metasomatism by hydrous silicic melts derived from subducted oceanic crust, *Nature*, *410*, 197–200, doi:10.1038/35065583.

Ranalli, G. (1995), *Rheology of the Earth*, 413 pp., Chapman and Hall, London.

Regenauer-Lieb, K., D. A. Yuen, and J. Branlund (2001), The initiation of subduction: Criticality by addition of water?, *Science*, *294*, 578–580, doi:10.1126/science.1063891.

Schmidt, M. W., and S. Poli (1998), Experimentally based water budgets for dehydrating slabs and consequences for arc magma generation, *Earth Planet. Sci. Lett.*, *163*, 361–379, doi:10.1016/S0012-821X(98)00142-3.

Scott, D. R., and D. J. Stevenson (1986), Magma ascent by porous flow, *J. Geophys. Res.*, *91*, 9283–9296, doi:10.1029/JB091iB09p09283.

Sizova, E., T. V. Gerya, M. Brown, and L. Perchuk (2010), Subduction styles in the Precambrian: Insight from numerical experiments, *Lithos*, *116*, 209–229, doi:10.1016/j.lithos.2009.05.028.

Somin, M., and G. Millán (1981), *Geology of the Metamorphic Complexes of Cuba [in Russian]*, Nauka, Moscow.

Sorensen, S. S. (1988), Petrology of amphibolite-facies mafic and ultramafic rocks from the Catalina Schist, southern California: Metasomatism and migmatization in a subduction zone metamorphic setting, *J. Metamorph. Geol.*, *6*, 405–435, doi:10.1111/j.1525-1314.1988.tb00431.x.

Sorensen, S. S., and M. D. Barton (1987), Metasomatism and partial melting in a subduction complex: Catalina Schist, southern California, *Geology*, *15*, 115–118, doi:10.1130/0091-7613(1987)15<115:MAPMIA>2.0.CO;2.

Sorensen, S. S., and J. N. Grossman (1989), Enrichment in trace elements in garnet amphibolites from a paleo-subduction zone: Catalina Schist, southern California, *Geochim. Cosmochim. Acta*, *53*, 3155–3177, doi:10.1016/0016-7037(89)90096-3.

Stern, R. J. (2002), Subduction zones, *Rev. Geophys.*, *40*(4), 1012, doi:10.1029/2001RG000108.

Stern, R. J. (2004), Subduction initiation: Spontaneous and induced, *Earth Planet. Sci. Lett.*, *226*, 275–292.

Thorkelson, D. J., and K. Breitsprecher (2005), Partial melting of slab window margins: Genesis of adakitic and non-adakitic magmas, *Lithos*, *79*, 25–41, doi:10.1016/j.lithos.2004.04.049.

Tsujimori, T., J. G. Liou, and R. G. Coleman (2005), Coexisting retrograde jadeite and omphacite in a jadeite-bearing lawsonite eclogite from the Motagua fault zone, Guatemala, *Am. Mineral.*, *90*, 836–842, doi:10.2138/am.2005.1699.

Tsujimori, T., V. B. Sisson, J. G. Liou, G. E. Harlow, and S. S. Sorensen (2006), Petrologic characterization of Guatemalan lawsonite–eclogite: Direct information on eclogitization of subducted oceanic crust in a cold subduction zone, in *Ultrahigh-Pressure Metamorphism: Deep Continental Subduction*, edited by B. H. Hacker, W. C. McClelland, and J. G. Liou, *Spec. Pap. Geol. Soc. Am.*, *403*, 147–168.

Ulmer, P. (2001), Partial melting in the mantle wedge-the role of H_2O in the genesis of mantle-derived 'arc-related' magmas, *Phys. Earth Planet. Inter.*, *127*, 215–232, doi:10.1016/S0031-9201(01)00229-1.

van Keken, P. E., B. Kiefer, and S. M. Peacock (2002), High-resolution models of subduction zones: Implications for mineral dehydration reactions and the transport of water into the deep mantle, *Geochem. Geophys. Geosyst.*, *3*(10), 1056, doi:10.1029/2001GC000256.